



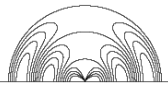
Title	Comprehensive study of plasmonic effects in organic solar cells
Author(s)	Sha, WEI; Choy, WCH; Chew, WC
Citation	The 34th Progress In Electromagnetics Research Symposium (PIERS 2013), Stockholm, Sweden, 12-15 August 2013.
Issued Date	2013
URL	http://hdl.handle.net/10722/189887
Rights	Creative Commons: Attribution 3.0 Hong Kong License

Comprehensive Study of Plasmonic Effects in Organic Solar Cells

*Wei E.I. Sha¹ (沙威), Wallace C.H. Choy¹ (蔡值豪),
and Weng Cho Chew² (周永祖)*

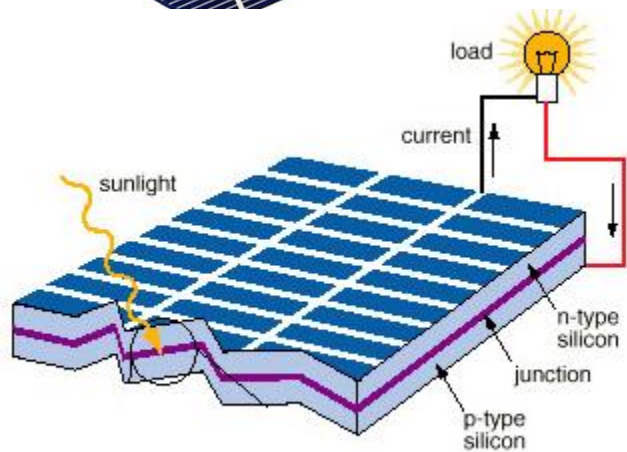
- 1. Department of Electrical and Electronic Engineering,
The University of Hong Kong, Hong Kong*
- 2. Department of Electrical and Computer Engineering,
University of Illinois, Urbana-Champaign,
Illinois 61801, USA*

Emails: chchoy@eee.hku.hk (W.C.H. Choy); w-chew@uiuc.edu (W.C. Chew)

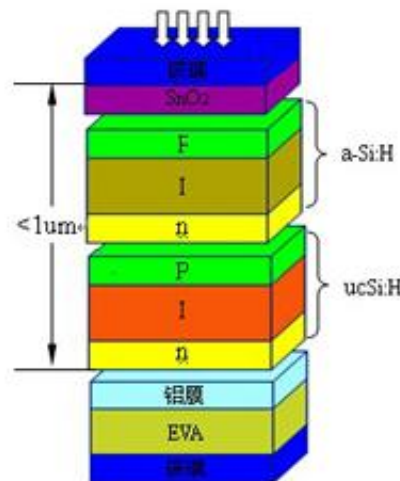


Organic Solar Cell (1)

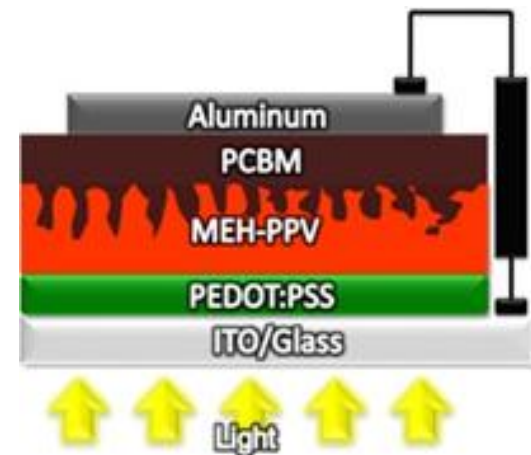
Advances of solar cell technology



monocrystalline silicon solar cell

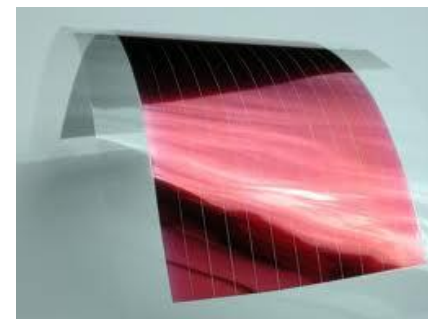


amorphous/polycrystalline silicon solar cell



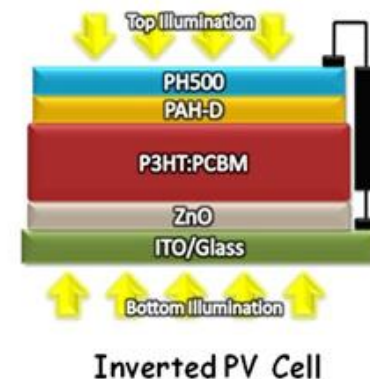
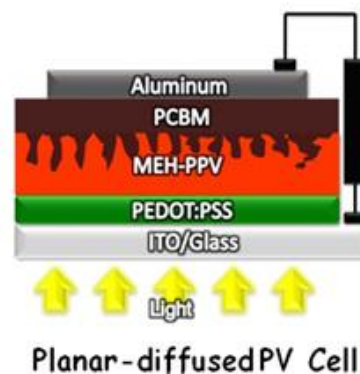
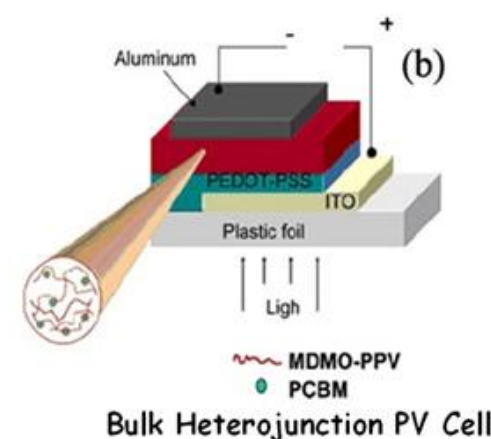
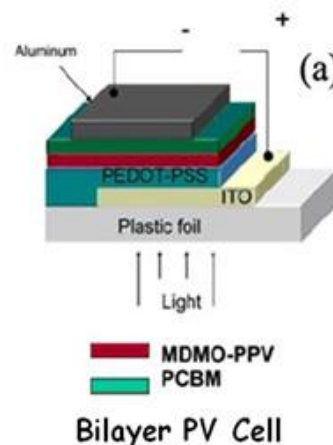
organic solar cell

Organic Solar Cell (2)



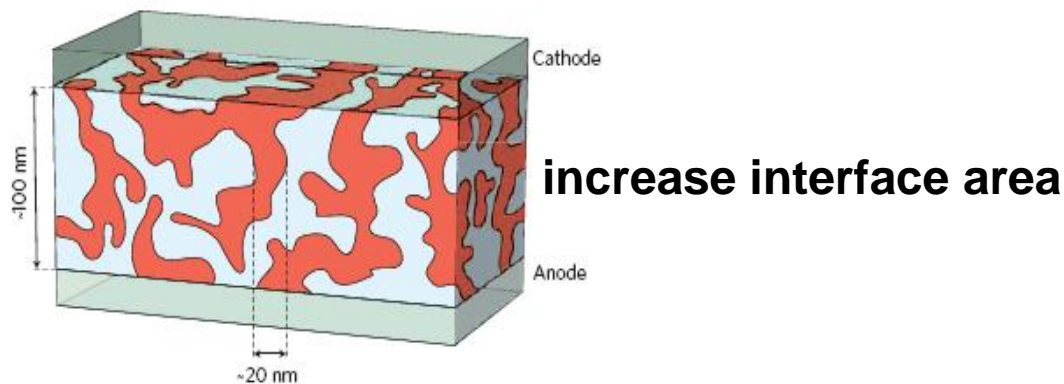
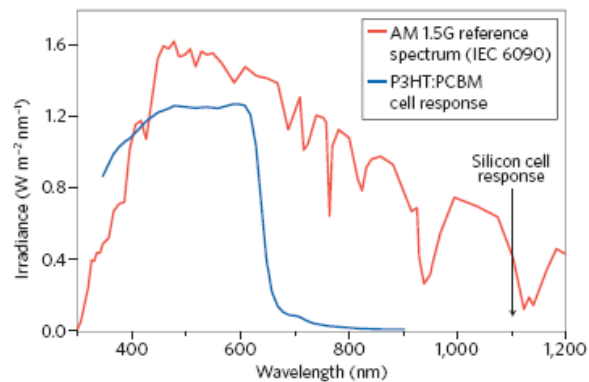
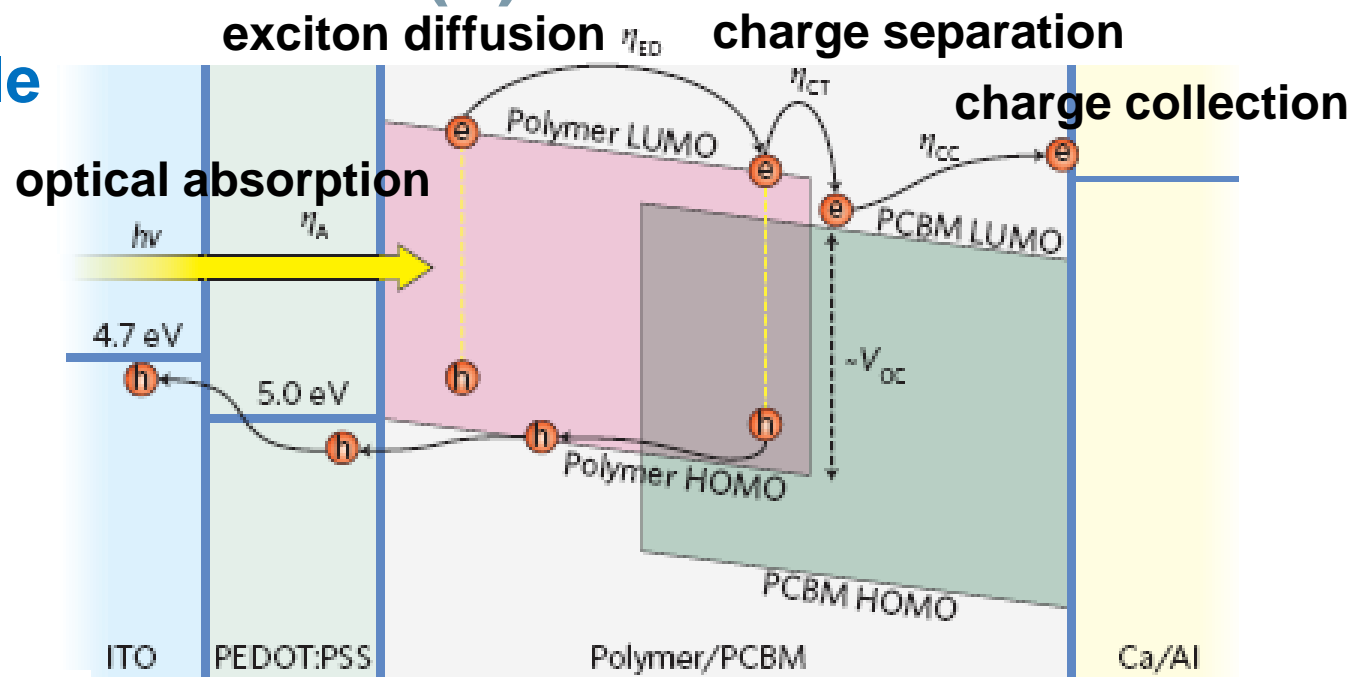
Thin-film organic solar cell

- ✓ *low-cost processing*
- ✓ *mechanically flexible*
- ✓ *large-area application*
- ✓ *environmentally friendly*
- X *low exciton diffusion length*
- X *low carrier mobility*



Organic Solar Cell (3)

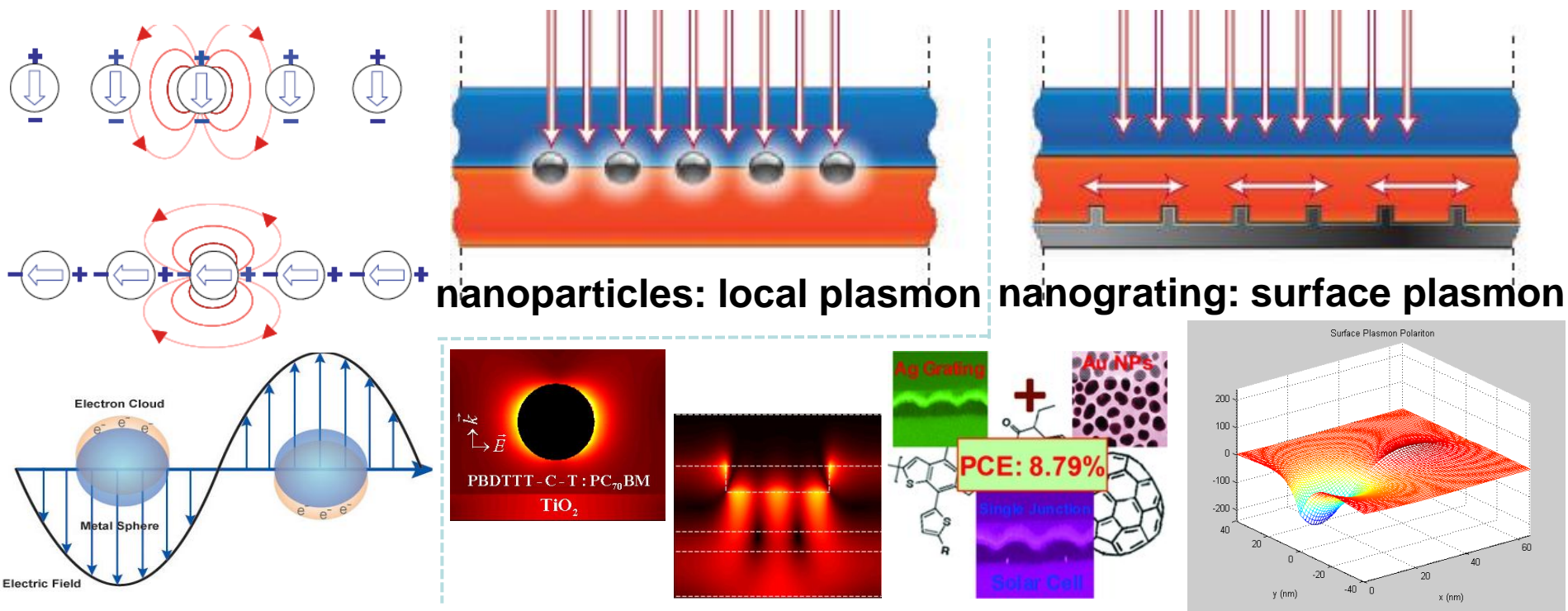
Working principle



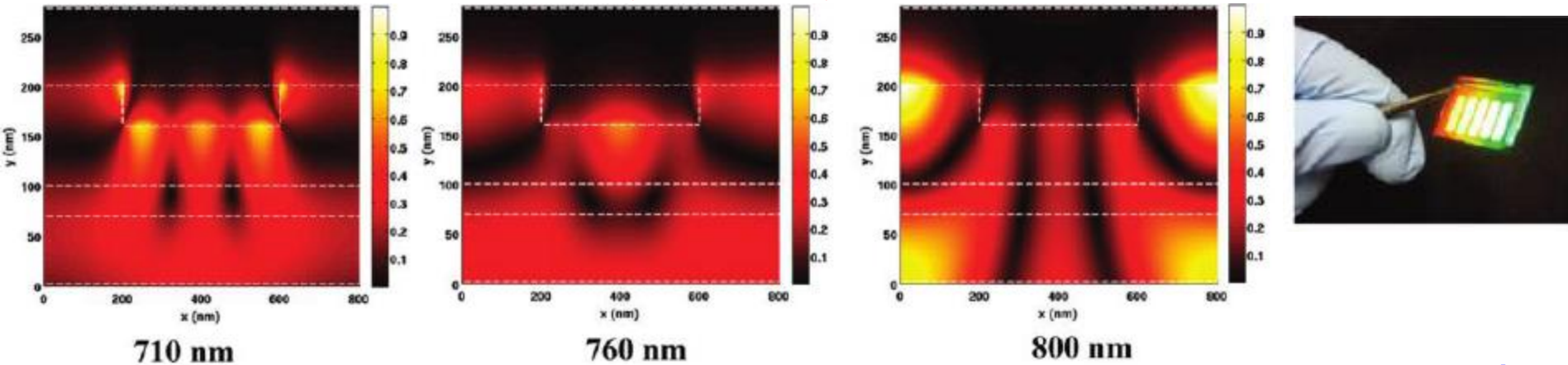
Plasmonic Organic Solar Cell

Why optical enhancement?

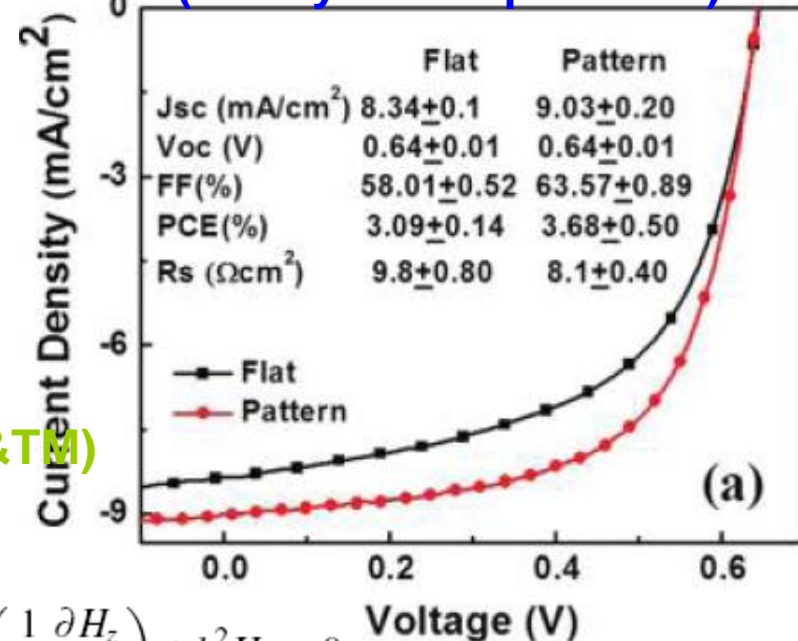
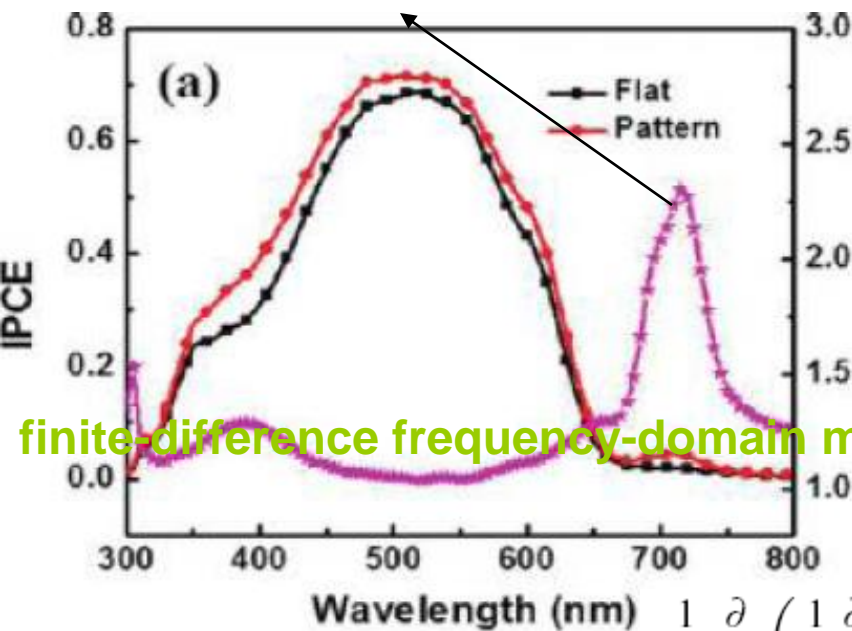
The thickness of the active layer must be smaller than the exciton diffusion length to avoid bulk recombination. As a result, the thin-film organic solar cell has poor photon absorption or harvesting. Plasmonic solar cell is one of emerging solar cell technologies to enhance the optical absorption.



X.H. Li, W.E.I. Sha, W.C.H. Choy, etc, J. Phys. Chem. C, 116(12), 7200-7206, 2012.



Plasmonic band edge boosted optical enhancement (theory and experiment)

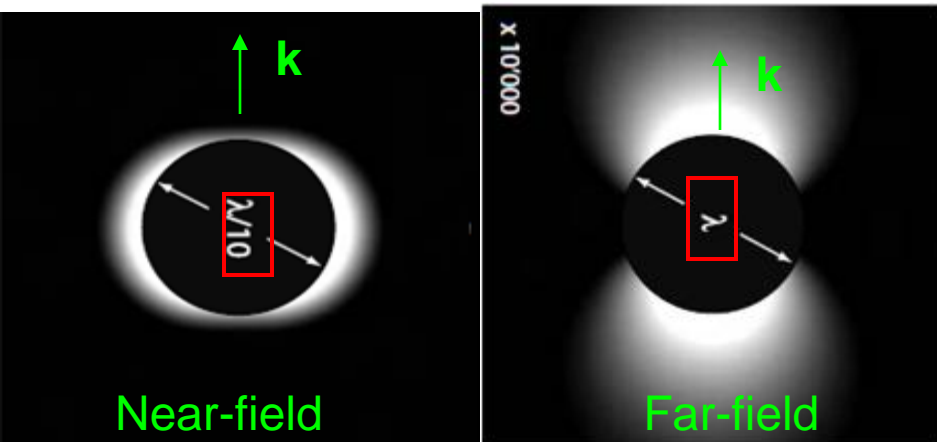
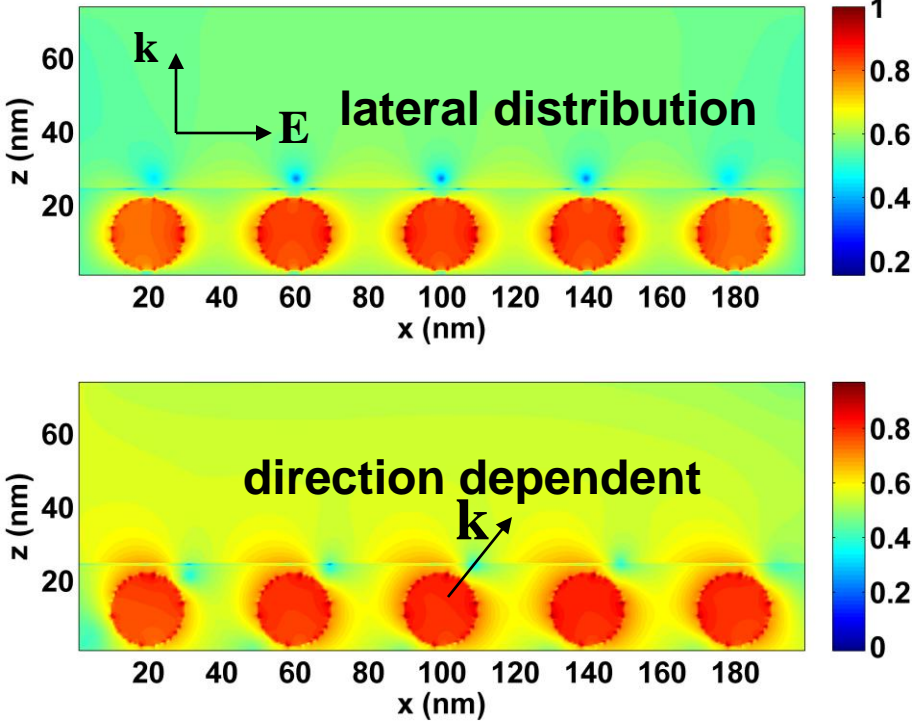


$$\frac{1}{\mu_r} \frac{\partial}{\partial x} \left(\frac{1}{\epsilon_r} \frac{\partial H_z}{\partial x} \right) + \frac{1}{\mu_r} \frac{\partial}{\partial y} \left(\frac{1}{\epsilon_r} \frac{\partial H_z}{\partial y} \right) + k_0^2 H_z = 0$$

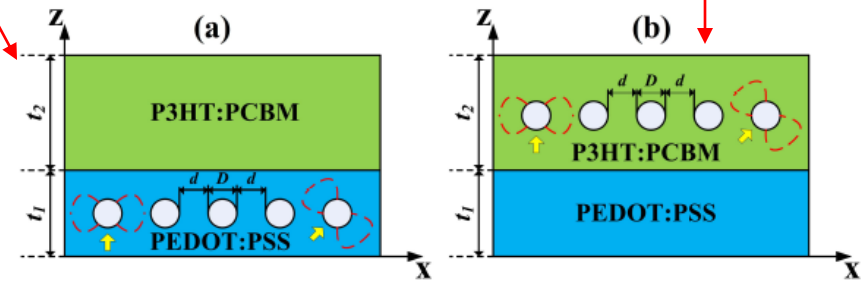
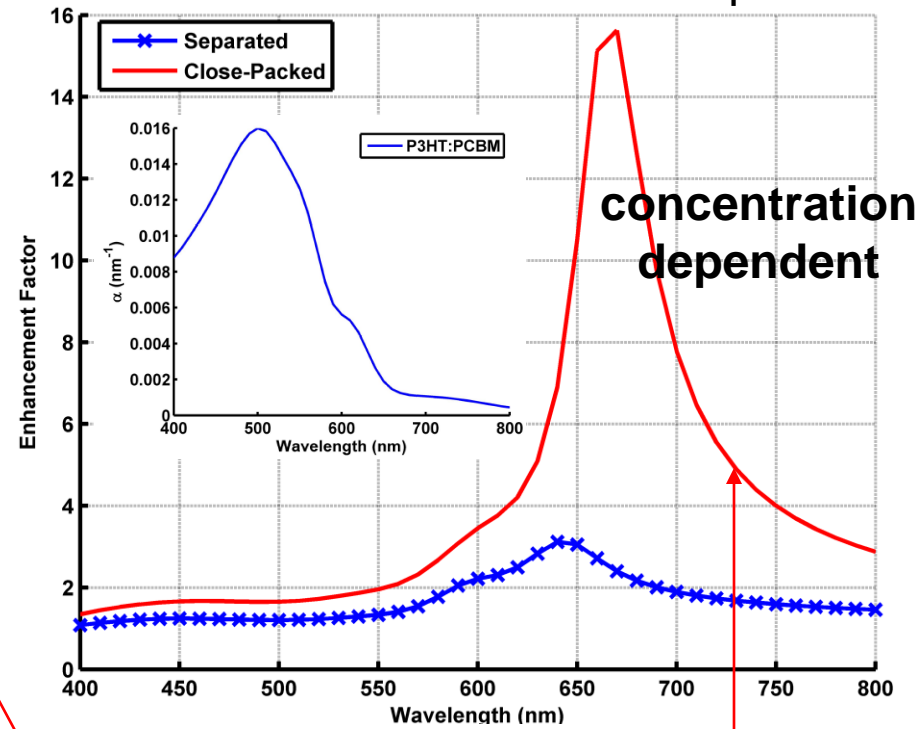


W.E.I. Sha, W.C.H. Choy, Y.P. Chen, and W.C. Chew, Appl. Phys. Lett., 99(11), 113304, 2011.

Bulk heterojunction polymer solar cell



2 fold increase in total absorption!



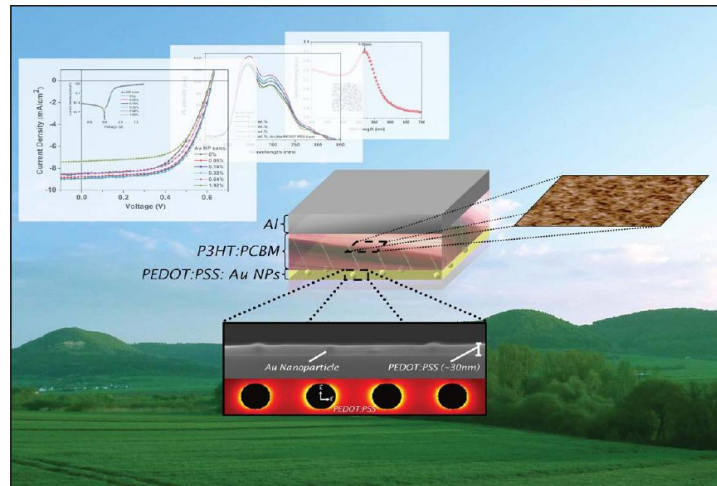
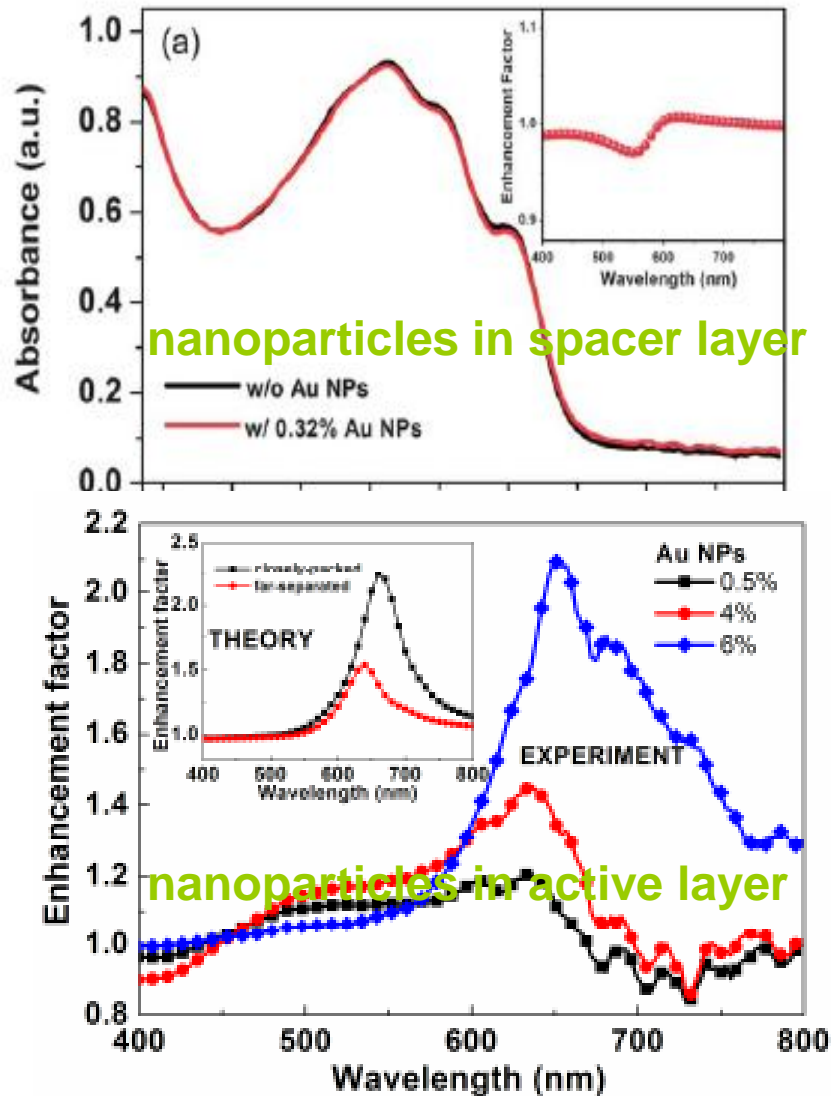
VIE-FFT method (BiCG-STAB)

$$\mathbf{E}^i(\mathbf{r}) = \frac{\mathbf{J}(\mathbf{r})}{j\omega(\epsilon(\mathbf{r}) - \epsilon_0)} + j\omega\mu_0 \int_v \overline{\mathbf{G}}(\mathbf{r}, \mathbf{r}') \cdot \mathbf{J}(\mathbf{r}') d\mathbf{r}'$$

Comparisons with experimental results

C.C.D. Wang, W.C.H. Choy, etc, *J. Mater. Chem.*, 22, 1206-1211, 2011.

D.D.S. Fung, L.F. Qiao, W.C.H. Choy, etc, *J. Mater. Chem.*, 21, 16349-16356, 2011.



**Selected as
Back Cover
and Hot
Article in
Journal of
Material
Chemistry**

Highlighting joint research results from the labs of Department of Electrical and Electronic Engineering, Faculty of Engineering, the University of Hong Kong and Centre for Optical and Electromagnetic Research, State Key Laboratory of Modern Optical Instrumentations, Zhejiang University.

Title: Optical and Electrical Properties of Efficiency Enhanced Polymer Solar Cells with Au Nanoparticles in PEDOT:PSS Layer

Efficiency improvement of polymer solar cells with Au nanoparticles doped into PEDOT:PSS is achieved and attributed to increased interfacial area between P3HT:PCBM and PEDOT:PSS instead of plasmonic effects. New device physics was unveiled, as the very strong LSPR near field of Au nanoparticles was found to distribute laterally along PEDOT:PSS and does not significantly improve P3HT:PCBM active layer absorption.

As featured in:

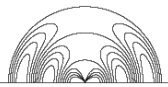


See Wallace C. H. Choy et al., *J. Mater. Chem.*, 2011, 21, 16349.

RSC Publishing

www.rsc.org/materials

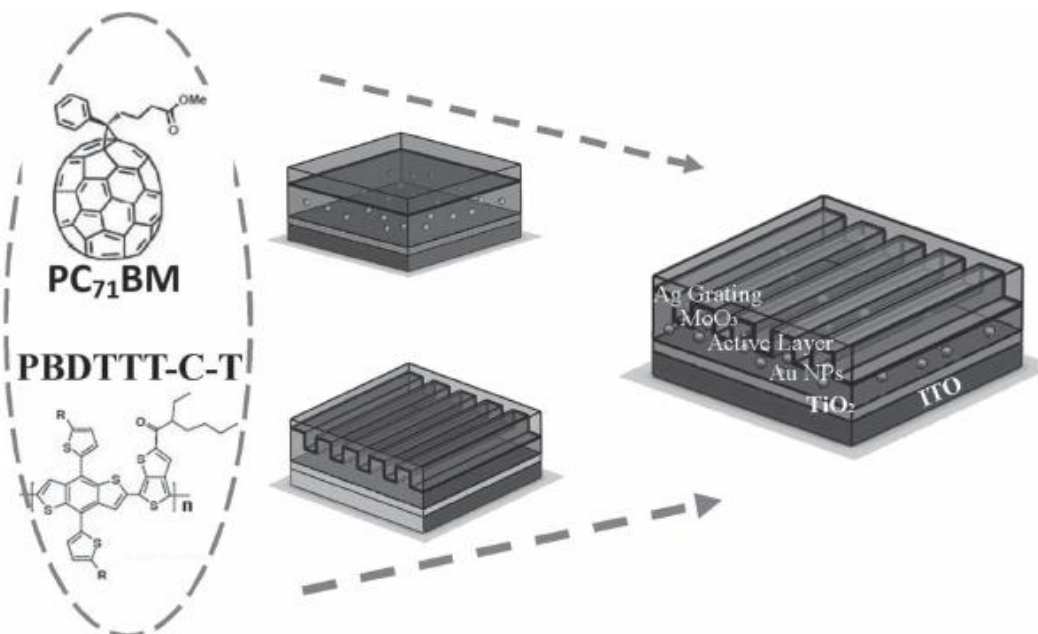
Registered Charity Number 207890



X.H. Li, W.C.H. Choy, L.J. Huo, F.X. Xie, W.E.I. Sha, B.F. Ding, X. Guo, Y.F. Li, J.H. Hou, J.B. You, and Y. Yang, Adv. Mater., 24, 3046–3052, 2012.

Dual Plasmonic Nanostructure (experimental results)
power conversion efficiency **8.79%**

Spin-coating+nanoimprinting



Ag Grating

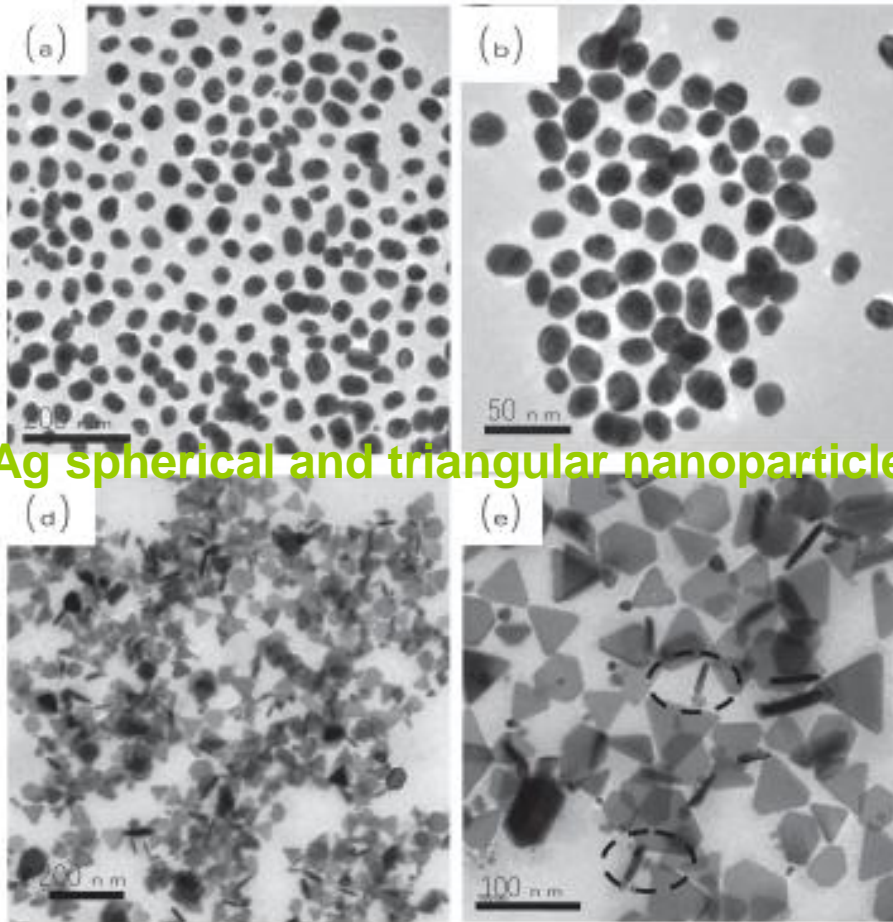
Au NPs

PCE: 8.79%

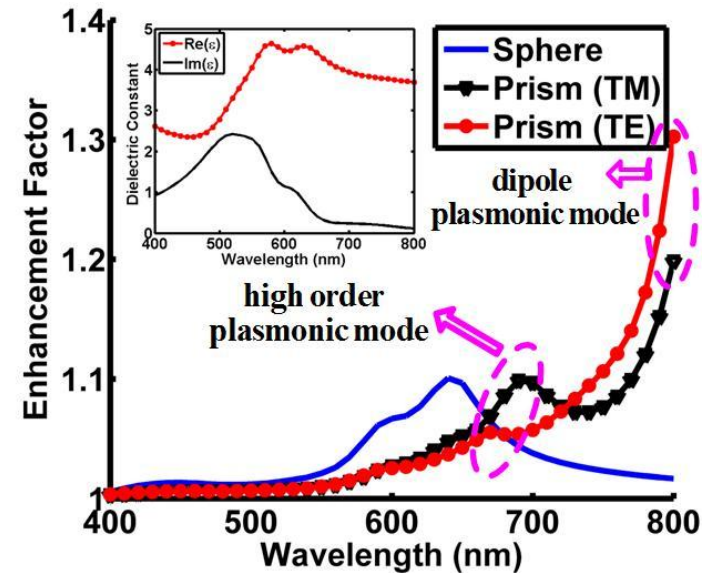
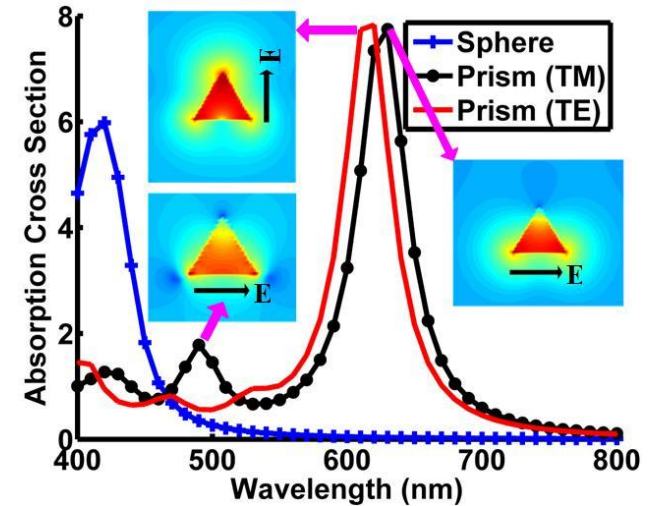
Single Junction Solar Cell

X.H. Li, W.C.H. Choy, H.F. Lu, W.E.I. Sha, and A.H.P Ho, Adv. Funct. Mater., 23(21), 2728–2735, 2013

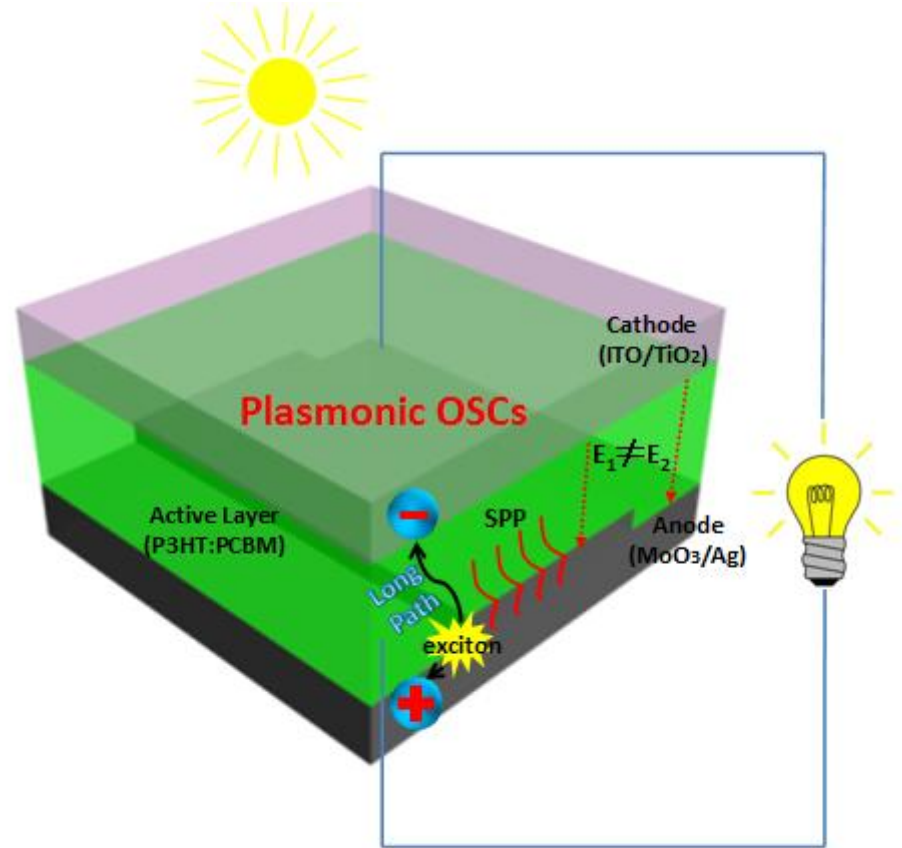
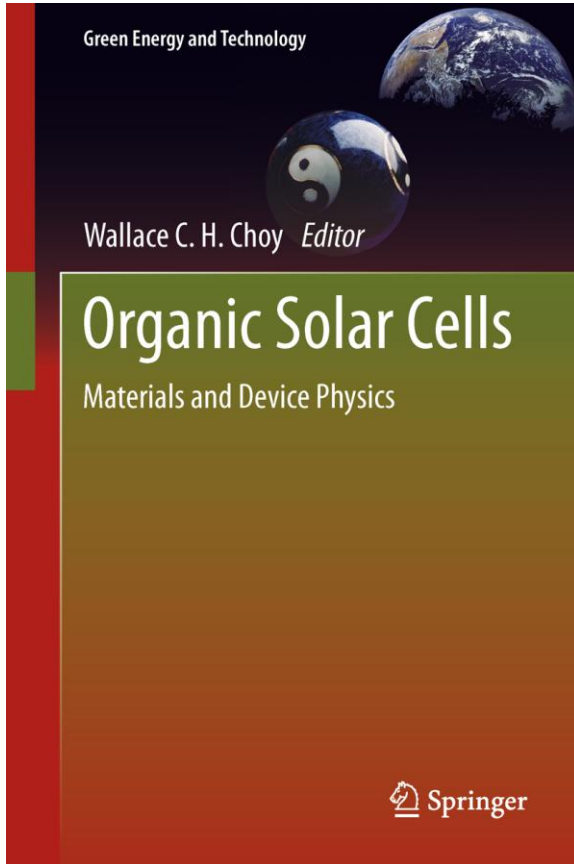
Shape-Dependent Broadband Plasmonic Resonances



Ag spherical and triangular nanoparticles



Could electrical properties of OSCs be affected by introducing the metallic nanostructures?



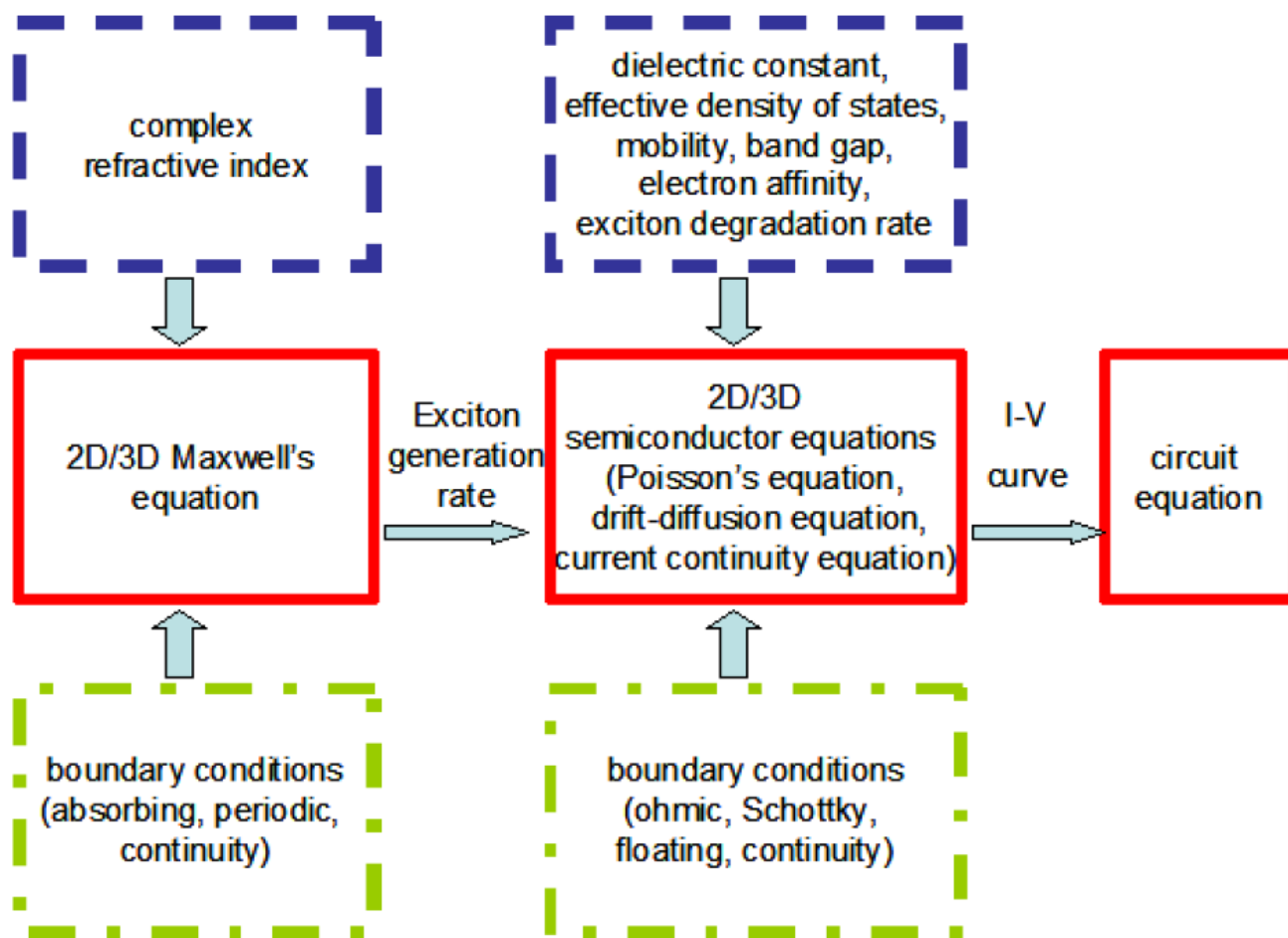
Wei E. I. Sha, Wallace C. H. Choy and Weng Cho Chew, "Theoretical Studies of Plasmonic Effects in Organic Solar Cells", Chapter 7, Organic Solar Cells: Materials and Device Physics, Pages 177-210, Wallace C.H. Choy (Ed.), ISBN 978-1-4471-4823-4, Springer, 2013.



Multiphysics Model (1)

W.E.I. Sha, W.C.H. Choy, Y.M. Wu, and W.C. Chew,
Opt. Express, 20(3), 2572-2580, 2012.*

Schematic diagram



Multiphysics Model (2)

Governing equations

frequency dependent permittivity

$$\nabla \times \mathbf{E} = -j\omega\mu_0 \mathbf{H}, \quad \nabla \times \mathbf{H} = j\omega\varepsilon(\omega)\mathbf{E}$$

Maxwell's equation

$$G(\mathbf{r}) = \int_{400}^{800} \frac{\lambda}{hc} A(\mathbf{r}, \lambda) d\lambda, \quad A(\mathbf{r}, \lambda) = \omega\varepsilon_0 n_r k_i |\mathbf{E}(\mathbf{r})|^2$$

generation rate

$$\nabla \cdot (\varepsilon \nabla \phi) = -q(p - n)$$

$$\frac{\partial n}{\partial t} = \frac{1}{q} \nabla \cdot (-q\mu_n n \nabla \phi + qD_n \nabla n) + QG - (1 - Q)R$$

$$\frac{\partial p}{\partial t} = -\frac{1}{q} \nabla \cdot (-q\mu_p p \nabla \phi - qD_p \nabla p) + QG - (1 - Q)R$$

semiconductor equations

electron density *electrostatic potential*
hole density *electrostatic dielectric constant* *bimolecular recombination rate*
mobility *Diffusion coefficients* *exciton dissociation probability*

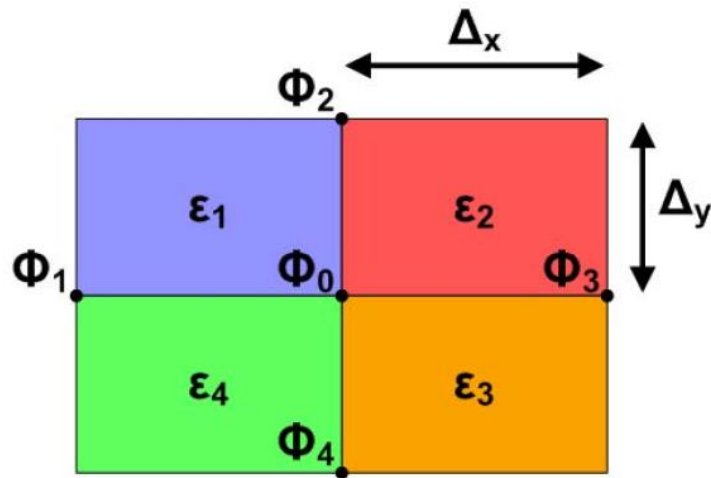


Multiphysics Model (3)

Unified finite difference method

optical properties

spatial step depends on the dielectric wavelength and skin depth of surface plasmons



2D wave equations: TE & TM

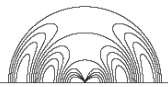
$$2 \left(\frac{1}{\Delta_x^2} + \frac{1}{\Delta_y^2} \right) \frac{\Phi_0}{\bar{\epsilon}} - k_0^2 \Phi_0 - \frac{\Phi_1 + \Phi_3}{\bar{\epsilon} \Delta_x^2} - \frac{\Phi_2 + \Phi_4}{\bar{\epsilon} \Delta_y^2} = 0, \quad \Phi = E_z$$

$$2 \left(\frac{1}{\Delta_x^2} + \frac{1}{\Delta_y^2} \right) \frac{\Phi_0}{\bar{\epsilon}} - k_0^2 \Phi_0 - \frac{\epsilon_1^{-1} + \epsilon_4^{-1}}{2\Delta_x^2} \Phi_1 - \frac{\epsilon_2^{-1} + \epsilon_3^{-1}}{2\Delta_x^2} \Phi_3 - \frac{\epsilon_1^{-1} + \epsilon_2^{-1}}{2\Delta_y^2} \Phi_2 - \frac{\epsilon_3^{-1} + \epsilon_4^{-1}}{2\Delta_y^2} \Phi_4 = 0, \quad \Phi = H_z$$

$$\bar{\epsilon} = \begin{cases} \frac{\epsilon_1 + \epsilon_2 + \epsilon_3 + \epsilon_4}{4}, & \Phi = E_z \\ 4(\epsilon_1^{-1} + \epsilon_2^{-1} + \epsilon_3^{-1} + \epsilon_4^{-1})^{-1}, & \Phi = H_z \end{cases}$$

periodic boundary conditions

stretched-coordinate perfectly matched layer



Multiphysics Model (4)

Poisson equation (Gummel's method)

electrical properties

spatial step depends on the Debye length

$$\begin{aligned} & \frac{1}{\Delta_x^2} \epsilon_{i+1/2,j}^d \phi_{i+1,j}^{t+1} + \frac{1}{\Delta_x^2} \epsilon_{i-1/2,j}^d \phi_{i-1,j}^{t+1} + \frac{1}{\Delta_y^2} \epsilon_{i,j+1/2}^d \phi_{i,j+1}^{t+1} + \frac{1}{\Delta_y^2} \epsilon_{i,j-1/2}^d \phi_{i,j-1}^{t+1} \\ & - \left(\epsilon_{i+1/2,j}^d + \epsilon_{i-1/2,j}^d + \epsilon_{i,j+1/2}^d + \epsilon_{i,j-1/2}^d \right) \left(\frac{1}{2\Delta_x^2} + \frac{1}{2\Delta_y^2} \right) \phi_{i,j}^{t+1} - \frac{n_{i,j}^t + p_{i,j}^t}{U_t} \phi_{i,j}^{t+1} \\ & = q(n_{i,j}^t - p_{i,j}^t) - \frac{n_{i,j}^t + p_{i,j}^t}{U_t} \phi_{i,j}^t \end{aligned}$$

drift-diffusion and continuity equations of electron (Scharfetter-Gummel scheme in spatial domain semi-implicit strategy in time domain)

$$\begin{aligned} \frac{n_{i,j}^{t+1} - n_{i,j}^t}{\Delta_t} &= Q_{i,j}^t G_{i,j} - (1 - Q_{i,j}^t) R_{i,j}^t + \frac{D_{i+1/2,j}^n}{\Delta_x^2} B \left(\frac{\phi_{i+1,j}^{t+1} - \phi_{i,j}^{t+1}}{U_t} \right) n_{i+1,j}^{t+1} \\ &+ \frac{D_{i-1/2,j}^n}{\Delta_x^2} B \left(\frac{\phi_{i-1,j}^{t+1} - \phi_{i,j}^{t+1}}{U_t} \right) n_{i-1,j}^{t+1} + \frac{D_{i,j+1/2}^n}{\Delta_y^2} B \left(\frac{\phi_{i,j+1}^{t+1} - \phi_{i,j}^{t+1}}{U_t} \right) n_{i,j+1}^{t+1} \\ &+ \frac{D_{i,j-1/2}^n}{\Delta_y^2} B \left(\frac{\phi_{i,j-1}^{t+1} - \phi_{i,j}^{t+1}}{U_t} \right) n_{i,j-1}^{t+1} - \left[\frac{D_{i+1/2,j}^n}{\Delta_x^2} B \left(\frac{\phi_{i,j}^{t+1} - \phi_{i+1,j}^{t+1}}{U_t} \right) \right. \\ &+ \frac{D_{i-1/2,j}^n}{\Delta_x^2} B \left(\frac{\phi_{i,j}^{t+1} - \phi_{i-1,j}^{t+1}}{U_t} \right) + \frac{D_{i,j+1/2}^n}{\Delta_y^2} B \left(\frac{\phi_{i,j}^{t+1} - \phi_{i,j+1}^{t+1}}{U_t} \right) \\ &\left. + \frac{D_{i,j-1/2}^n}{\Delta_y^2} B \left(\frac{\phi_{i,j}^{t+1} - \phi_{i,j-1}^{t+1}}{U_t} \right) \right] n_{i,j}^{t+1} \end{aligned}$$

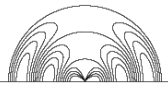
scaling unit

cm	$\max \{ \text{DOS} \}^{1/3}$
s	10^{12}
V	1
C	$\frac{1}{1.602 \times 10^{-19}}$
K	$\frac{1}{300}$

Dirichlet and Neumann boundary conditions

time step for stable algorithm

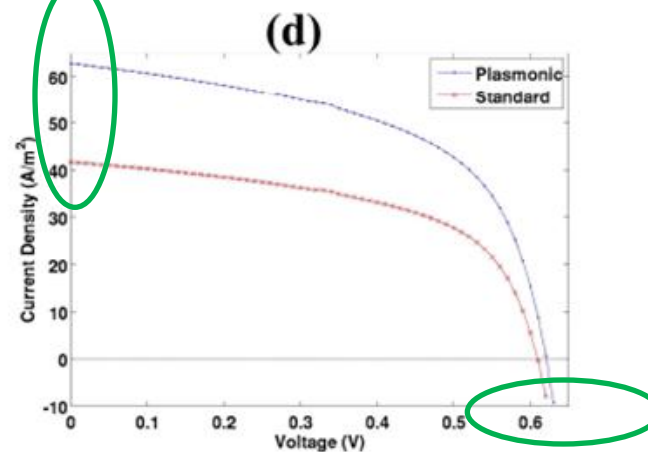
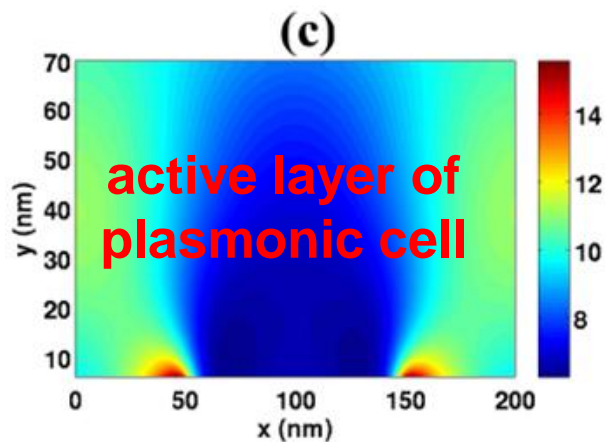
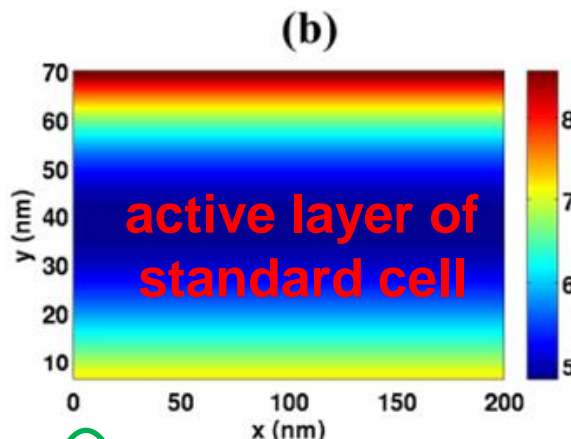
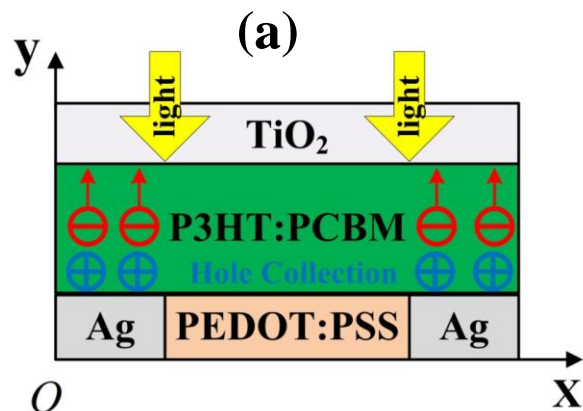
$$\Delta_t < \min \left(\frac{C\epsilon}{\mu_n \cdot n + \mu_p \cdot p} \right)$$



Multiphysics Model (5)

Beyond optical absorption enhancement: facilitating hole collection!

schematic pattern of nanostrip plasmonic cell



Model settings

- active layer thickness 70 nm
- periodicity 200 nm
- PEDOT:PSS width 100 nm
- anode ohmic
- cathode barrier height 0.2 eV
- hole mobility 0.1*electron mobility
- effective band gap 1.1 eV

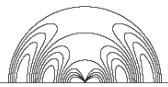
Multiphysics Model (6)

Characteristic parameters

Plasmonic	J_{sc} (A/m ²)	V_{oc} (V)	MP (W)	FF	PCE (%)
	62.84	0.62	21.47	0.55	2.15
Standard	J_{sc} (A/m ²)	V_{oc} (V)	MP (W)	FF	PCE (%)
	41.67	0.61	14.03	0.55	1.40

Plasmonic	V (V)	J (A/m ²)	\langle Diss \rangle (%)	\langle Rec loss \rangle (%)
SC	0	62.84	66.96	2.62
MP	0.48	44.73	58.97	14.55
OC	0.62	0	55.47	80.88
Standard	V (V)	J (A/m ²)	\langle Diss \rangle (%)	\langle Rec loss \rangle (%)
SC	0	41.67	66.96	3.18
MP	0.47	30.42	59.19	14.93
OC	0.61	0	55.75	81.91

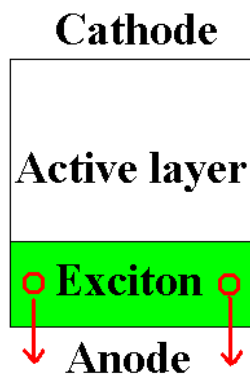
- **reduce recombination loss**
- **increase short-circuit current**
- **improve open-circuit voltage**
- **boost power conversion efficiency**



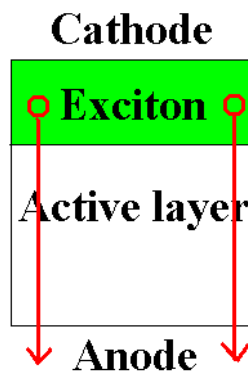
Multiphysics Model (7)

Dummy case for further illustrating physics (hole transport and collection)

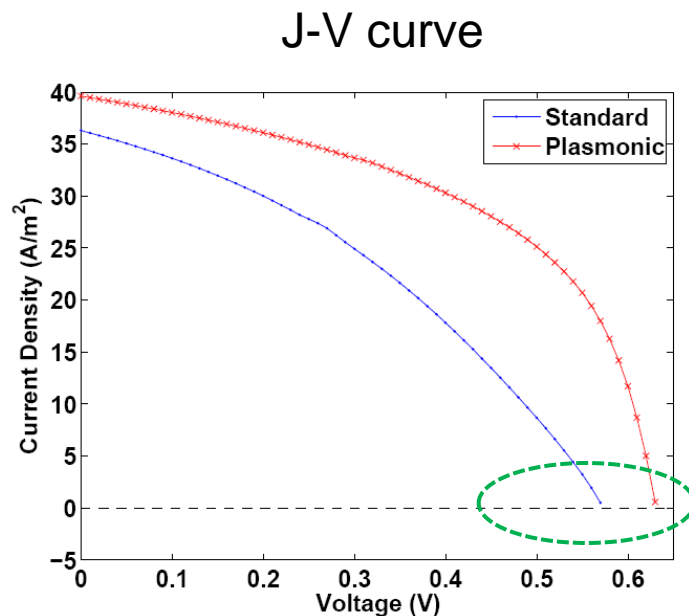
$$G_{grating} = \begin{cases} G_c, & d_3 \leq y \leq d_3 + L_g \\ 0, & \text{else} \end{cases}$$



$$G_{planar} = \begin{cases} G_c, & d_3 + d_2 - L_g \leq y \leq d_3 + d_2 \\ 0, & \text{else} \end{cases}$$



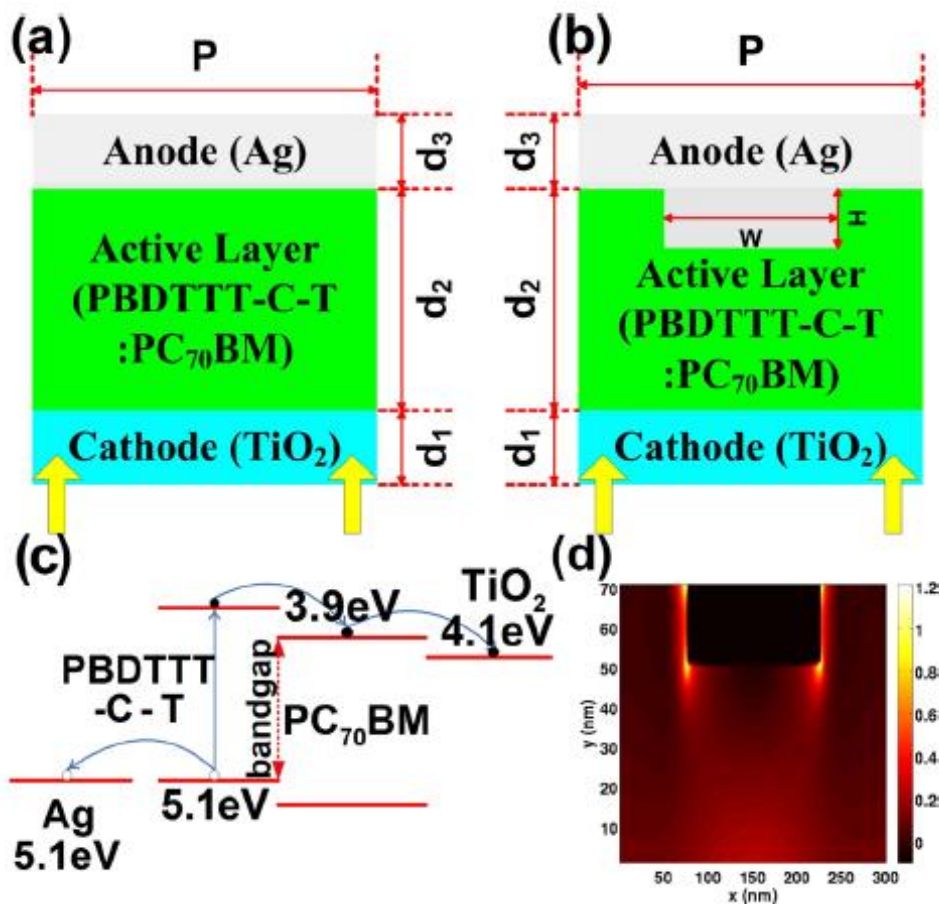
hole mobility is set to be two order of magnitude lower than electron mobility



inhomogeneous exciton generation significantly affects fill factor and open-circuit voltage

Multiphysics Model (8)

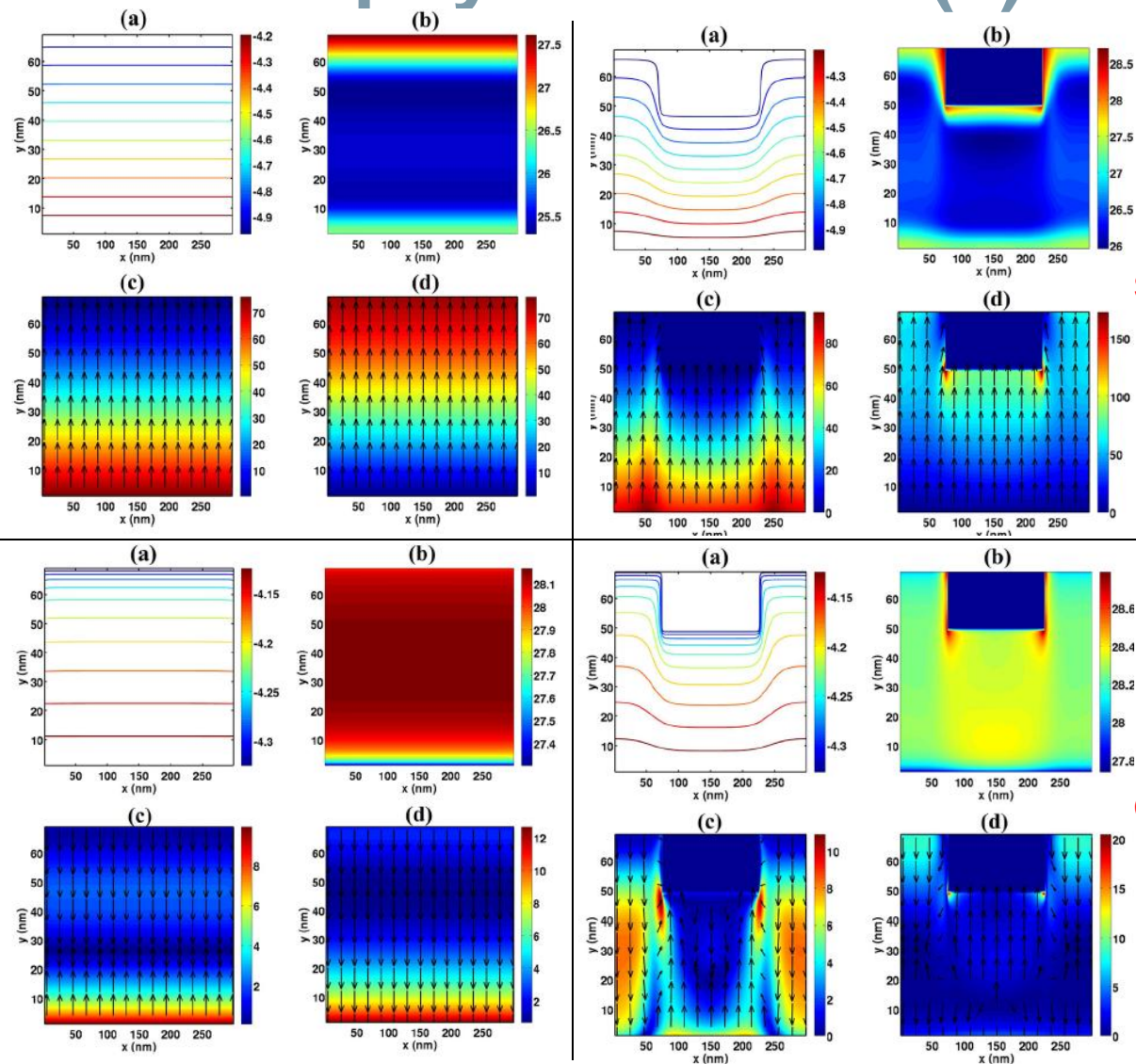
The nanograting structure v.s. flat standard structure



Simulation parameters

E_g	1.2 eV
μ_n	$7.4 \times 10^{-7} \text{ m}^2 / (\text{V} \cdot \text{S})$
μ_p	$7.4 \times 10^{-8} \text{ m}^2 / (\text{V} \cdot \text{S})$
N_c	$2.5 \times 10^{19} \text{ cm}^{-3}$
N_v	$2.5 \times 10^{19} \text{ cm}^{-3}$
ϵ^d	$3.4\epsilon_0 \text{ F/m}$
a	1.12 nm
k_T	$3 \times 10^5 \text{ s}^{-1}$
ψ_b^n	0.2 eV
ψ_b^p	0 eV

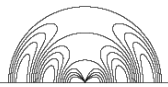
Multiphysics Model (9)



short-circuit

(a) equipotential lines; (b) recombination rate; (c,d) electron and hole current densities.

open-circuit



Multiphysics Model (10)

$$FF = \frac{P_{MAX}}{P_T} = \frac{I_{MP} \cdot V_{MP}}{I_{SC} \cdot V_{OC}}$$

The grating anode induces nonuniform optical absorption and inhomogeneous internal E-field distribution. Thus uneven photocarrier generation and transport are formed in the plasmonic OSC leading to the dropped FF.

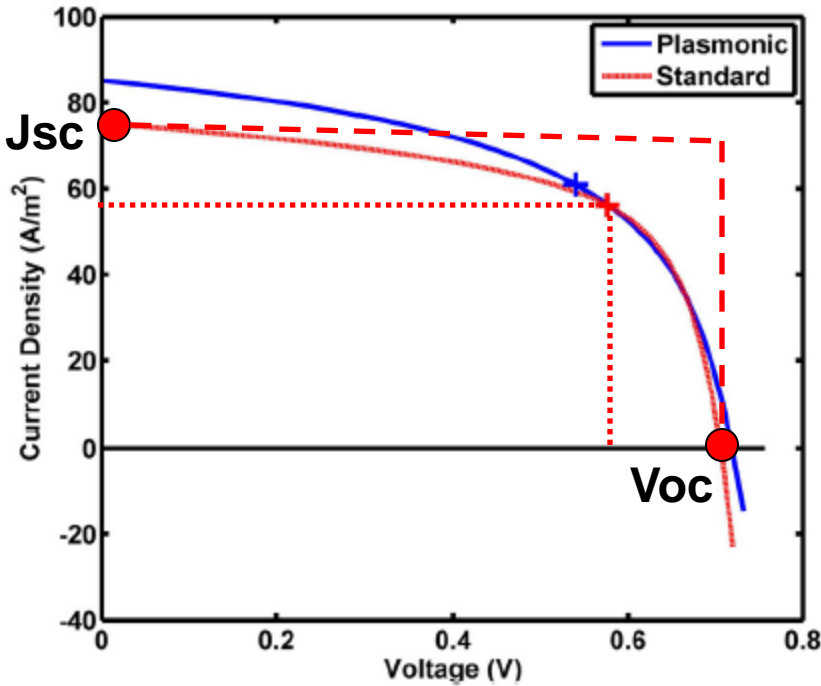


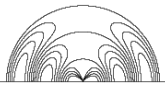
TABLE II. The characteristic parameters of the standard and plasmonic OSCs involving short-circuit J_{sc} , open-circuit voltage V_{oc} , MP, FF, and PCE.

	J_{sc} (A/m ²)	V_{oc} (V)	MP (W)	FF (%)	PCE (%)
Standard	75.18	0.706	32.34	60.91	3.23
Plasmonic	85.12	0.719	32.91	53.77	3.29

	SC (Diss)	SC (Rec)	MP (Diss)	MP (Rec)	OC (Diss)	OC (Rec)
Standard (%)	69.83	0.88	62.34	9.19	59.69	82.56
Plasmonic (%)	70.52	2.5	63.38	16.63	59.63	92.75

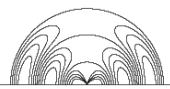
recombination and exciton dissociation

W.E.I. Sha, W.C.H. Choy, and W.C. Chew, Appl. Phys. Lett., 101, 223302, 2012.*



Conclusion

- ✓ Environmentally friendly organic solar cell (OSC), which has a bright outlook to meet the urgent demand in clean energy, draws much attention in recent years due to their merits of large-area production, low-cost processing and mechanical flexibility. Proposing and optimizing new device architectures plays a key role in designing high-performance OSCs.
- ✓ A multiphysics study carries out on plasmonic OSCs by solving Maxwell's equations and semiconductor (Poisson, drift-diffusion, and continuity) equations simultaneously with a unified finite-difference framework.
- ✓ Nonuniform distributions of optical near-fields induced by plasmonic nanostructures will significantly affect the carrier transport in OSCs. Besides their optical effects, the electrical effects induced by plasmonic resonances will open up a new way to design emerging plasmonic organic photovoltaics.



Acknowledgement

Thanks for your attention!

